From the Mary Anne Mc Phail Equine Performance Center, Department of Large Animal Clinical Sciences, East Lansing, USA

Changes in trunk shape and center of mass location in horses during walking

S. NAUWELAERTS and H.M. CLAYTON

received January 21, 2009
accepted for publication August 24, 2009

Keywords: center of mass, horse, locomotion, shape changes, walk.

Summary

It was the aim of this study to describe trunk deformations and their effect on the location of the trunk center of mass during walking.

Each of 6 horses walked at 10 velocities within the range 0.7-1.9 m/s. A mesh of forty markers equally spaced around the trunk and markers on the hooves were tracked using a motion analysis system. Marker coordinate data were used to determine changes in trunk shape in relation to the timing of limb movements. The position of the center of mass determined from a standing file (CM_{rigid}) was assumed to remain in a constant position relative to markers on the horse's spine during locomotion. In order to take account of trunk deformation during walking, $CM_{deformable}$ was calculated as the centroid of the marker mesh in a local horse-fixed coordinate system.

During hind limb protraction, trunk length decreased while trunk height and width increased, especially in the abdominal region. Mean amplitude of the difference between the positions of $CM_{deformable}$ and CM_{rigid} was 5.8 ± 0.2 mm (mean ± SEM) in the vertical direction, 32.8 ± 1.2 mm in the longitudinal and 46.9 ± 1.3 mm in the transverse directions. Amplitudes increased with speed and were horse dependent.

Inter-individual variation complicates the development of correction routines to compensate for the effects of trunk deformation on calculating the location of the trunk CM based on the standing position. Estimates of trunk CM location can, however, be improved using extra markers distributed over the trunk segment.

Abbreviation: CM = center of mass

Schlüsselwörter: Körperschwerpunkt, Pferd, Bewegung, Formveränderung, Schritt.

Zusammenfassung

Veränderungen der Rumpfform und des Schwerpunktes bei Pferden im Schritt

Ziel der Studie war es, die Verformungen des Rumpfes und deren Effekt auf die Lokalisierung des Rumpfschwerpunktes im Schritt zu untersuchen.

6 gesunde Pferde wurden bei je 10 Geschwindigkeiten zwischen 0,7 und 1,9 m/s getestet. Ein Netz aus 40 Markern um den Rumpf und an den Hufen wurde mittels eines Bewegungsanalysesystems aufgenommen. Die Koordinaten der Marker wurden genutzt, um die Rumpfform in Relation zu den Gliedmaßenbewegungen zu bestimmen. Es wurde angenommen, dass die im Stehen bestimmte Position des Körperschwerpunktes (CM_{rigid}) während der Bewegung in einer konstanten relativen Position zu Markern am Rücken verbleibt. Um die Rumpfdeformation im Schritt zu bestimmen, wurde der $CM_{deformable}$ als Schwerpunkt des Markernetzes in einem örtlich fixiertem Koordinatensystem berechnet.

Während der Protraktion der Hintergliedmaßen sinkt die Rumpflänge, während die Rumpfhöhe und -weite besonders in der Abdominalregion steigen. Die mittlere Amplitude der Differenz zwischen den Positionen von $CM_{deformable}$ und CM_{rigid} war 5,8 ± 0,2 mm ($\bar{x}$ ± SEM) in der vertikalen Richtung, 32,8 ± 1,2 mm in der longitudinalen und 46,9 ± 1,3 mm in der transversalen Richtung. Die Amplitude stieg mit der Geschwindigkeit und war abhängig von den Pferden.

Die interindividuelle Variation erschwert die Entwicklung von Korrekturroutinen zur Kompensation der Effekte der Rumpfdeformation bei der Berechnung des im Stehen kalkulierten Rumpfschwerpunktes. Die Abschätzung der Rumpfschwerpunktlokalisation kann jedoch mittels zusätzlicher, über dem Rumpf verteilter, Marker verbessert werden.

Introduction

Knowledge of equine biomechanics has advanced rapidly over the past decennia by using technology adapted from human biomechanics. Similarly to the latter field, one of the primary technical factors limiting progress is the measurement of skeletal movement from markers placed on the skin (ANDRIACCHI and ALEXANDER, 2000). Skin movement with respect to the underlying bones can be corrected based on algorithms developed from studies using bone-fixed markers (WEEREN and BARNEVELD, 1986; KHUMSAP et al., 2004; SHA et al., 2004). Since this is an invasive technique, it is impractical to use bone-fixed markers in every study and studies using this technique tend to be based on a small number of animals performing within a limited range of gaits and speeds, which may create a bias if the corrections are applied under different circumstances. A way to avoid this type of bias is to fit marker data onto a body template that consists of interconnected rigid bodies in an inverse kinematics analysis (BOGERT et al., 1990; BUCHNER et al., 2000; BOBBERT et al., 2007). This technique relies heavily on the assumption that segments are rigid and therefore do not deform during locomotion.

DOI: 10.4112-10-91

In a previous paper, we demonstrated that the rigidity assumption is violated in the horse trunk segment during both walking and trotting and that errors arising due to trunk deformation have significant consequences for mechanical energy estimates during locomotion (NAUWELAERTS et al., 2009). This study was designed to describe how trunk shape changes in relation to footfall patterns during walking; and to measure the subsequent effect on estimations of center of mass (CM) position of the trunk segment.

Material and methods

The study was performed with approval by the institutional animal ethics committee as protocol 10/07-154-00.

Experimental setup

Animals

Data were obtained from 6 sound horses (3 Arabians, 1 Thoroughbred cross, 1 Warmblood and 1 Quarter Horse), with an age (mean ± SD) of 10 ± 5 years and a body mass of 502 ± 98 kg, representing a variety in body shapes and sizes.

Motion capture

45 reflective cubes of 6 mm were attached to each horse using double-sided tape. The trunk was represented by 40 skin markers attached in a regular grid pattern and placed geometrically rather than in respect to anatomical structures. The grid consisted of 5 spine markers, equally spaced between the highest point on the withers and the caudal lumbar region; 5 ventral markers aligned below the spine markers; and 3 rows of 5 markers evenly spaced between the spine markers and the ventral markers on each side of the body (Fig. 1). The marker at the height of the stifle was put at an offset to ensure visibility throughout the entire stride. Additional markers were placed on the forehead and on the lateral side of each hoof to determine footfall patterns.

3-dimensional kinematic data were collected in the global coordinate system using 8 Eagle infrared cameras recording at 120 Hz using EVaRT 5.0.4 software (Motion Analysis, Santa Rosa, CA). The cameras surrounded a capture volume of 3 m by 2 m by 2 m. An L-shaped calibration frame consisting of 4 markers that could be seen by all cameras defined a global coordinate system. A T-shaped wand with 3 markers was used to test the calibration dynamically. The mean error associated with measuring the length between 2 wand markers that were 500 mm apart was 0.6 ± 0.9 mm.

Each experiment started with recording a static 60 Hz trial of the horse standing square. A stick figure was built to facilitate automated recognition of the markers. Horses were warmed up in and accustomed to the experimental arena by walking them through the capture volume. During data collection, horses were led in hand through the calibrated volume and the cranial spine marker was used to determine average speed of each trial, which was reported immediately after completion of the trial. Data collection continued until 10 trials had been recorded representing the entire range of speeds over which each horse was willing to walk.

Data Analysis

For each horse, 10 walking sequences within the speed range of 0.7 to 1.9 m/s were analyzed. A trial consisted of a single stride starting with contact of the right forelimb. The axes of a local coordinate system for the trunk segment were determined based on the trunk dimensions: X is longitudinal and positive cranially, Z is vertical and positive upward, and Y is transverse, mutually perpendicular to the X and Z axes, and positive to the left. The origin of the local coordinate system was defined in the center of the volume of the mesh formed by the 40 trunk markers in the standing trial. A system of 3 linear equations based on the relationships between the center of this volume and the coordinates of the 5 spine markers was defined for each horse (NAUWELAERTS et al., 2009). These equations, which showed only small variations between different standing trials, were used to calculate the position of the center of the trunk volume based on the positions of the spine markers in the walking trials. The origin of this local coordinate system that moves with the horse and that represents the center of mass of the rigid trunk segment will be named CM_{rigid} in the rest of the manuscript.

The volume encompassed by the linear mesh of 40 trunk markers, which represents the shape of the deformable trunk, was calculated in 3DSMAX 9 (Autodesk, Inc., San Rafael, CA). The coordinates of the CM of the deformable trunk were determined assuming uniform density of the segment. This is referred to as $CM_{deformable}$.

Height and width of the trunk segment were calculated separately for the 5 rings of trunk markers. Height was the distance between the spine marker and the corresponding ventral marker and width was measured between the 2 middle marker rows. Length of the trunk segment was calculated as the distance between the centers of the cranial and caudal rings of markers. Changes in trunk dimensions were expressed as a percentage of the standing values. Graphs plotting the differences between the locations of CM_{rigid} and $CM_{deformable}$ were generated for each trial and values representing the minimal and maximal separations of CM_{rigid} and $CM_{deformable}$ during each stride were calculated and the difference between them was the amplitude of the difference in CM position due to trunk deformation along the 3 axes of the local coordinate system.

Statistics

To test overall amplitudes of displacement of the $CM_{deformable}$ calculated from the volume in a local coordinate system through the spine markers relative to CM_{rigid} determined from the standing file, a MANCOVA model was constructed in SPSS 16.0 (SPSS Inc., Chicago). The amplitudes of the difference between CM_{rigid} and $CM_{deformable}$ were compared by including volume as a fixed effect. Effects of walking speed were adjusted as a covariate. 2-factor interaction effects between horse and volume were included. In addition, we tested for individual differences by including the horse as a fixed effect in the multivariate analyses, while in the univariate tests the horse was added as a random effect. By creating box plots by fixed effect, significant effects could be evaluated for their biological relevance.

DOI: 10.4112-10-91

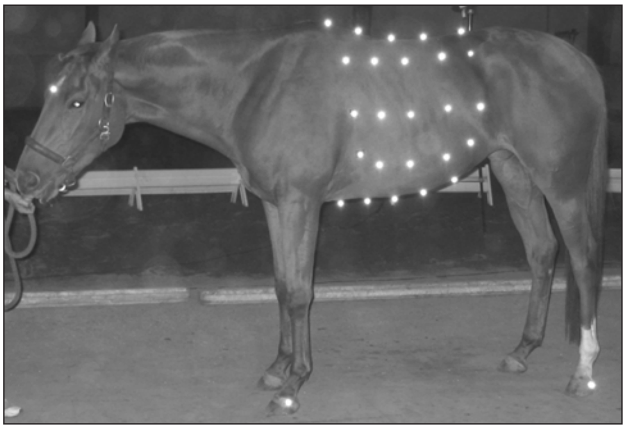

Fig. 1: Lateral view on the horse with grid of reflective markers; note that the marker caudal to the olecranon is slightly offset dorsally to avoid interference with the movements of the forelimb. The rows of markers are equal distances apart in the dorsoventral direction although the curvature of the ribcage makes it difficult to appreciate this in the lateral view.

Results

Changes in trunk shape

Changes in trunk height increased in a cranial to caudal direction (Fig. 2): at the level of the first ring of markers around the ribcage the height changed by about 2 % of maximal height, while the 2 caudal levels of markers around the abdomen showed height increases of 4 to 5 %. The profiles of the height changes for the abdominal markers were sinusoidal with height peaks coinciding with the times when $CM_{deformable}$ had moved maximally caudally and laterally. Similar patterns were found for the widths measured at different locations along the craniocaudal axis.

Effect of trunk deformation

The origin of the local coordinate system attached to the horse's spine (CM_{rigid}) and the CM calculated as the centroid of the trunk volume ($CM_{deformable}$) did not move together throughout the walking stride (Fig. 3). The smallest amplitude of this difference was in the vertical direction (5.8 ± 0.2 mm [mean ± SEM]): $CM_{deformable}$ was consistently slightly higher than CM_{rigid}. Larger differences were present in the longitudinal (amplitude 32.8 ± 1.2 mm) and transverse (46.9 ± 1.3 mm) directions. $CM_{deformable}$ had its maximal cranial displacement relative to CM_{rigid} in the middle of the forelimb stance phase, then moved caudally until late in forelimb stance (Fig. 3). In the transverse direction, the movements of $CM_{deformable}$ relative to CM_{rigid} showed 4 peaks: the 2 displacement peaks to the right occurred around the times of contact of the right forelimb and the subsequent contact of the left hind limb. During the left hind braking phase, the relative position of $CM_{deformable}$ moved rapidly to the left (Fig 3). The same pattern occurred in mirror image after the left forelimb contacted the ground.

Effect of speed

The general MANCOVA showed a significant effect of speed on the error amplitude in all 3 directions when corrected for individual differences. The effect of speed (m/s) was most obvious in the craniocaudal direction (slope of 25), while mediolateral and vertical amplitudes (mm) had slopes of 4 and 1, respectively (Fig. 4).

Inter-individual differences

In the general MANCOVA, the effect of individual horse on the difference in amplitude between $CM_{deformable}$ and CM_{rigid} was significant in all 3 directions. This could be due to either the absolute average amplitude being horse-dependent or the rate at which amplitude changes with speed varying from horse to horse. Average inter-individual differences were small. Maximal differences between the horses are larger in the transverse direction (25 mm) than in longitudinal (8 mm) and vertical (3 mm) directions, because the overall amplitudes are largest in this direction. No clear patterns with body mass and stride length were found: only the average amplitude of CM in the vertical direction correlated with body mass.

Discussion

Several mechanisms can cause the position of the CM of the trunk to shift relative to the position of the CM extrapolated from measurements on a cadaver trunk. These mechanisms can be divided into 2 major categories: changes in trunk dimensions or changes in trunk density distribution. We focused this paper on the effect of changes in trunk dimensions on the position of the trunk CM, but will address the ways in which density changes can affect CM position later in the discussion.

It is not surprising that height and width of the trunk show larger changes in the abdominal region where the body wall is relatively compliant compared with the cranial thorax which is bounded by the ribcage. Some of the changes in trunk dimensions may be driven by intervertebral flexion/extension. For example, flexion at the lumbosacral joint causes pelvic rotation that shortens the trunk in the craniocaudal direction (YOUNG et al., 1992). During walking, the thoracolumbar spine flexes in the early part of hind limb protraction and, at the same time, bends laterally so the trunk is convex toward the grounded hind limb (FABER et al., 2000). Intervertebral joint flexions likely contribute to the shortening of trunk length and, in order to accommodate the visceral mass, the height and width of the trunk increase in the abdominal region (LICKA et al., 2001; 2009). Compared with the trot, the thoracolumbar intervertebral joints undergo a larger range of motion at walk (FABER et al., 2000, 2001), and this is reflected by larger changes in trunk dimensions during walking than trotting (NAUWELAERTS and CLAYTON, 2009).

After hind limb contact, the trunk rolls towards the side of the grounded hind limb and $CM_{deformable}$ is displaced toward that side throughout hind limb stance. The first peak in transverse displacement coincides with forelimb contact

DOI: 10.4112-10-91

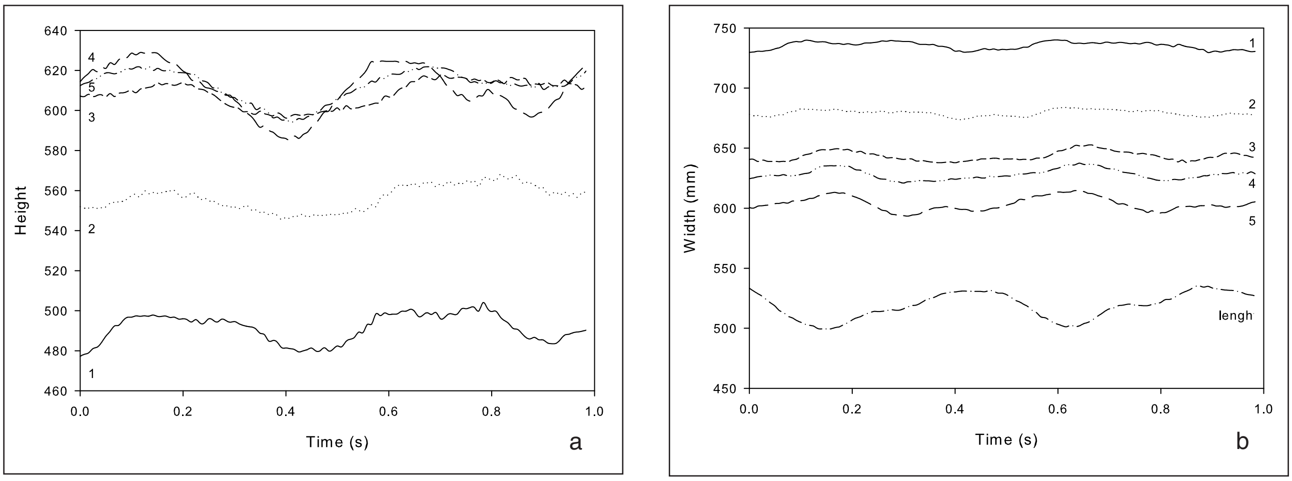

Fig. 2: a: Changes in trunk dimensions during the locomotor cycle at walk; changes in vertical trunk dimension at 5 levels along the trunk (height 1: most cranial to height 5: most caudal) and changes in trunk length; b: changes in trunk width at 5 levels along the trunk (width 1: most cranial to width 5: most caudal)

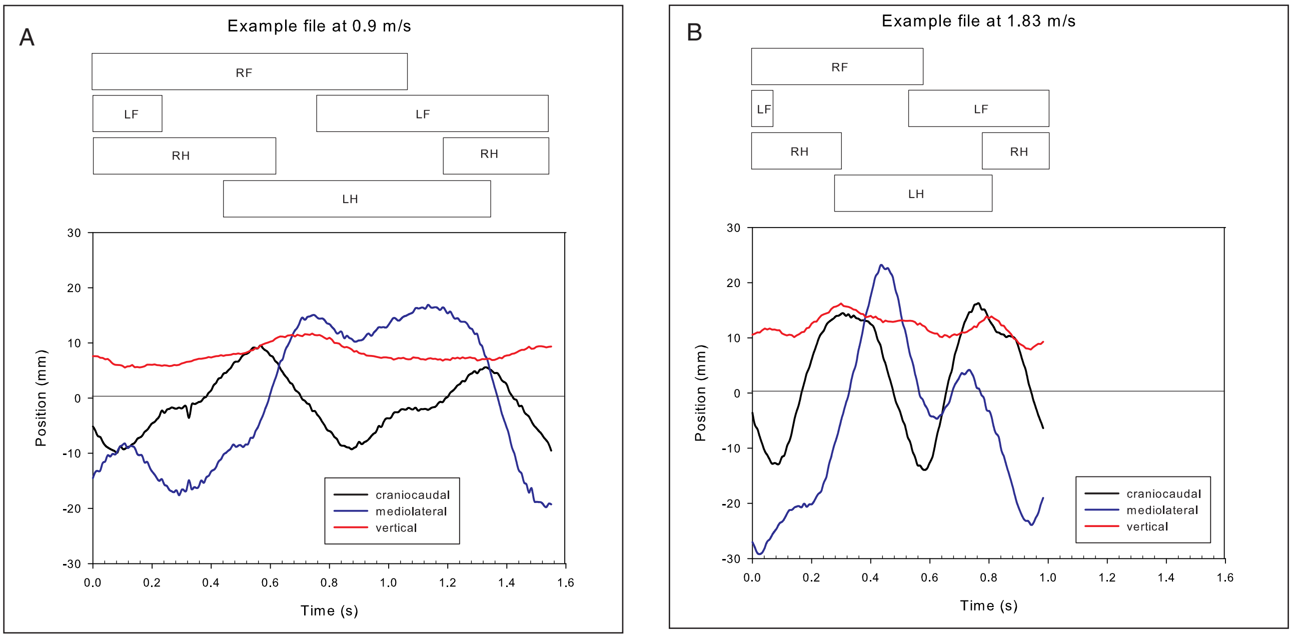

Fig. 3: Patterns of displacement of $CM_{deformable}$ calculated from the trunk volume in a local coordinate system relative to CM_{rigid} which is at the origin of the local coordinate system calculated from equations describing the relative position of the CM of the trunk volume of a standing horse based on 5 spine markers; X is the longitudinal axis (positive cranially), Y is transverse (positive left) and Z is vertical (positive up). Data are for a horse walking at (A) 0.9 m/s and (B) 1.83 m/s. Footfall patterns are shown as rectangular boxes representing the stance phases (RF= right front, LF= left front, RH= right hind, LH= left hind).

and is followed by a movement back toward the midline that may be a consequence of impact loading compressing the thorax dorso-ventrally on the side of the grounded forelimb (YOUNG et al., 1992). Since the forelimbs are set down out of phase during walking, the left and right sides are compressed alternately causing the ribcage to bulge in the opposite direction, which moves $CM_{deformable}$ transversely away from the grounded forelimb early in its stance phase. After the impact phase, $CM_{deformable}$ moves back toward the supporting forelimb as the opposite forelimb pushes off. Thus, the transverse profile is double humped on each side with the thorax and abdomen of the horse moving as a unit.

Activation of the abdominal muscles may stabilize the trunk and reduce abdominal inertial movements (ROBERT et al., 2001; LICKA et al., 2009) as has been demonstrated in the cat by CARLSON et al. (1979). Since $CM_{deformable}$ is consistently higher than CM_{rigid} during walking compared with standing, it can be assumed that the abdominal muscles are engaged to elevate the ventral abdominal wall. Stabilization of the trunk by the abdominal muscles may also explain why the assumption of a rigid trunk works

DOI: 10.4112-10-91

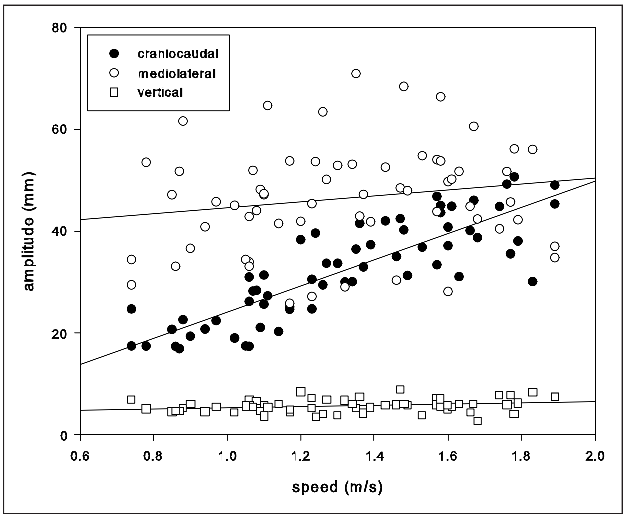

Fig. 4: Effect of speed on the error amplitudes in the position of $CM_{deformable}$ relative to CM_{rigid} along the 3 directions of the local coordinate system fixed in the spine

in the vertical direction: deviations from the rigid approach are small (<1 cm). Since the error in the vertical direction is small, it is possible to obtain accurate estimates of the vertical ground reaction forces from kinematic data (BOBBERT et al., 2007). On the other hand, activation of the abdominal muscles does not prevent the belly from swaying sideways: amplitudes in the mediolateral direction are considerably larger during walking than during trotting (NAUWELAERTS and CLAYTON, 2009).

It is possible that vertical movements of the head and neck (KHUMSAP et al., 2002) contribute to craniocaudal shifts in the position of $CM_{deformable}$ relative to CM_{rigid}. The head is highest during tripedal support with 2 forelimbs and 1 hind limb in stance, which corresponds with the most caudal displacement of $CM_{deformable}$. The head is lowest during tripedal support with 2 hind limbs and 1 forelimb in stance, which corresponds with the most cranial displacement of $CM_{deformable}$. The equations to estimate the position of CM_{rigid} were based on a standing trial during which the horse's head was in an intermediate position. In static studies, it has been shown radiographically that lowering the head and neck is associated with cranial displacement of the skin over the withers relative to the underlying thoracic spinous processes (RHODIN, 2008). Our interpretation of the craniocaudal shifts from the rigid segment approach is that lowering the head and neck in early forelimb stance stretches the skin of the cranial trunk forwards, whereas raising the head and neck in the later part of forelimb stance releases tension and allows the skin to slide back. Vertical movements of the head are larger during walking than during trotting, which fits our observation that longitudinal shifts of $CM_{deformable}$ are larger at walk than trot (NAUWELAERTS and CLAYTON, 2009). Furthermore, maximal and minimal head heights and head excursions are positively correlated with walking velocity (KHUMSAP et al., 2002), which offers an explanation for the strong effect of speed on movements in the craniocaudal direction.

This study investigated how changes in trunk shape could potentially affect the position of the trunk CM. However, changes in the density distribution of the trunk can also influence CM position. At rest, the equine diaphragm is concave when relaxed and flattens caudally when activated causing air to fill the lungs as the liver and abdominal viscera shift caudally, thereby decreasing the density of the cranial part of the trunk. Thus breathing is likely to affect CM position in the longitudinal direction. During locomotion, inertially driven movements of the visceral piston are responsible for locomotor respiratory coupling, especially during cantering but there is no consistent phase-coupling relationship between breathing and forelimb movements in walking horses (AINSWORTH et al., 1996), making it difficult to estimate the effect of breathing and visceral displacement on trunk CM position during walking. Future studies may use different techniques to investigate the density distribution within the equine thorax and abdomen.

In conclusion, changes in the shape of the trunk volume during walking alter the position of the trunk CM. When extrapolating the position of the trunk CM from cadaver data, one should be aware of this extra source of error, separate from the measurement error of the cadaver CM. Furthermore, the amount of inter-individual variation complicates theoretical correction routines. Estimates of trunk CM location can, however, be improved using extra markers distributed over the trunk segment.

Acknowledgements
This study was funded by the McPhail Endowment. The authors thank LeeAnn Kaiser, Robert Malinowski, Lila Zarski, Whitney Allen and Nicole Smith for assistance during data collection and analysis.

References

AINSWORTH, D.M., EICKER, S.W., NALEVANKO, M.E., DUCHARME N.G., HACKETT R.P., SNEDDED, K. (1996): The effect of exercise on diaphragmatic activation in horses. Respiratory Physiology **106**, 35-46.

ANDRIACCHI, T.P., ALEXANDER, E.J. (2000): Studies of human locomotion: past, present and future. Journal of Biomechanics **33**, 1217-1224.

BUCHNER, H.H.F., OBERMULLER, S., SCHEIDL, M. (2000): Body centre of mass movement in the sound horse. Veterinary Journal **160**, 225-234.

BOBBERT, M.F., ALVAREZ, C.B.G., WEEREN, P.R. van, ROEPSTORFF L., WEISHAUPT, M.A. (2007): Validation of vertical ground reaction forces on individual limbs calculated from kinematics of horse locomotion. The Journal of Experimental Biology **210**, 1885-1896.

CARLSON, H., HALBERTSMA, J., ZOMLEFER, M. (1979): Control of the trunk during walking in the cat. Acta Physiologica

Scandinavica **105**, 251-253.
FABER, M., SCHAMHARDT, H., WEEREN, R. van, JOHNSTON, C., ROEPSTORFF, L., BARNEVELD, A. (2000): Basic three-dimensional kinematics of the vertebral column of horses walking on a treadmill. American Journal of Veterinary Research **61**, 399-406.
FABER, M., JOHNSTON, C., SCHAMHARDT, H., WEEREN, R. van, ROEPSTORFF, L., BARNEVELD. A. (2001): Basic three-dimensional kinematics of the vertebral column of horses trotting on a treadmill. American Journal of Veterinary Research **62**, 757-764.
KHUMSAP, S., LANOVAZ, J.L., CLAYTON, H.M. (2004): Verification of skin-based markers for 3-dimensional kinematic analysis of the equine tarsal joint. Equine Veterinary Journal **36**, 655-658.
KHUMSAP, S., CLAYTON, H.M., LANOVAZ, J.L., BOUCHEY, M. (2002): Effect of walking velocity on forelimb kinematics and kinetics. Equine Veterinary Journal (Suppl. 34), 325-329.
LICKA, T., FREY, A., PEHAM, C. (2009): Electromyographic activity of the longissimus dorsi muscles in horses when walking on a treadmill. Veterinary Journal **180**, 71-76.
LICKA, T., PEHAM, C., ZOHMANN, E. (2001) Range of back movment at the trot in horses without back pain. Equine Veterinary Journal (Suppl. 33), 150-153.
NAUWELAERTS, S., CLAYTON, H.M. (2009): Trunk deformation in the trotting horse. Equine Veterinary Journal **41**, 203-206.
NAUWELAERTS, S., KAISER, L., MALINOWSKI, R., CLAYTON, H.M. (2009): Effects of trunk deformation on trunk center of mass mechanical energy estimates in the moving horse, *Equus caballus*. Journal of Biomechanics **42**, 308-311.
RHODIN, M. (2008): A biomechanical analysis of relationship between the head and neck postion, vertebral column and limbs in the horse at walk and trot. Thesis, Swedish University of Agricultural Sciences, Uppsala.
ROBERT, C., VALETTE, J.P., DENOIX, J.M. (2001): The effects of treadmill inclination and speed on the activity of three trunk muscles in the trotting horse. Equine Veterinary Journal **33**, 466-472.
SHA, D.H., MULLINEAUX, D.R., CLAYTON, H.M. (2004): Three-dimensional analysis of patterns of skin displacement over the equine radius. Equine Veterinary Journal **36**, 665-670.
BOGERT, A.J. van den, WEEREN, P.R. van, SCHAMHARDT, H.C. (1990): Correction for skin displacement errors in movement analysis of the horse. Journal of Biomechanics **23**, 97-102.
WEEREN, P.R. van, BARNEVELD, A. (1986): A technique to quantify skin displacement in the walking horse. Journal of Biomechanics **19**, 879-884.
YOUNG, I.S., ALEXANDER, R., WOAKES, A.J., BUTLER, P.J., ANDERSON, L. (1992): The synchronization of ventilation and locomotion in horses (*Equus caballus*). The Journal of Experimental Biology **166**, 19-31.

Author's address:
Sandra Nauwelaerts, PhD., Hilary M. Clayton, BVMS, PhD, MRCVS, D202 Veterinary Medical Center, East Lansing, MI 48824-1314, USA.
e-mail: nauwelae@cvm.msu.edu

DOI: 10.4112-10-91